Proceedings of 14th IOE Graduate Conference
Peer Reviewed
Year: 2023 Month: December Volume: 14
ISSN: 2350-8914 (Online), 2350-8906 (Print)

Dynamic Analysis of Pipe Conveying Fluid with excited supports

Jaybabu Mahato [a], Mahesh Chandra Luintel [b]

[a] *Department of Automobile and Mechanical Engineering, Thapathali Campus, IOE, Tribhuvan University, Nepal*
[b] *Department of Mechanical and Aerospace Engineering, Pulchowk Campus, IOE, Tribhuvan University, Nepal*
[a] mahato.jay1010@gmail.com, [b] mcluintel@ioe.edu.np

Abstract
This paper examines the dynamic analysis of fluid-conveying pipes with excited supports, considering various end conditions and materials. At first the fluid acceleration is derived through the dynamic method and then the governing equation of motion is derived via Newtonian method. Furthermore, Galerkin method is used to discretized the dynamic equation and numerical analysis is performed via fourth-order-Rung-kutta method. In given end conditions, the transverse deflection, deflection at different location throughout the length, bending moment at different fluid velocity are studied for two different pipe materials for two boundary conditions i.e pinned-pinned and pinned-free. The conclusion so made in this paper indicates that the deflection as well as bending moment increases with fluid velocities which suggests as the fluid speed increases, the pipe's stiffness decreases. Similarly the bending moment magnitudes for both pinned-pinned and pinned-free ends for both pipe materials is seen maximum at middle position in comparison to at either ends.

Keywords
Newtonian method, excited vibration, flow-induced vibration, transverse deflection

1. Introduction

Pipelines used for fluid transportation are commonly employed in different areas like Hydropower, water irrigation, petroleum transportation, nuclear power plant etc. The dynamic response caused due to fluid flow and fluid-structure interaction, however, often caused serious vibration and threatens the normal and safe operation of the entire systems. Such failures are becoming main reason to economy losses in worldwide. This is the reason why so many studies are being performed in flow induced vibration and many dynamical model are being formed [1, 2, 3].

The governing equation of a fluid-conveying pipe is typically obtained using generalized Hamilton's principle, the finite element method, or the Newtonian method. [4, 5].

The numerical solution techniques, the extended dynamic model pipe and dynamic characters for more specific problems, are becoming the areas for study. Ivan Grant [6], Utilized a finite-element method to simulate and solve the dynamic responses of the pipeline under two different sets of boundary conditions, namely simply-supported and cantilevered. Y L Zhang et al. [7] used the he Lagrange principle, the Ritz method to derive equation of motion. Additionally, employed the Eulerian approach along with the concept of fictitious loads to account for kinematic corrections in the analysis of geometrically non-linear vibrations. The model was subsequently tested experimentally to examine the vibrational characteristics of the fluid-conveying pipe, of simply supported, subjected to initial axial tensions. The same geometric parameters, used in experiments are also used in this research paper.

Similarly, Naguleswaran [8] used Rayleigh–Ritz as well as Fourier series solutions for the investigation of the lateral vibration of end conditions of the pipe conveying fluid with consideration of axial tension and internal pressure.This study explores the natural frequency equations for fluid-structure interaction in a pipeline conveying fluid with support at both ends, employing a direct approach [9]. The method, derived from Ferrari's technique, is applied to solve quartic equations. The dynamic equation for the fluid-conveying pipeline is derived using Hamilton's variation principle based on Euler-Bernoulli Beam theory. Natural frequency equations and critical flow velocity equations for pipelines with support at both ends are obtained using the separation of variables method and the modified Ferrari's method. These equations are then compared with natural frequency results obtained using the eliminated element-Galerkin method [10].

The effect of coriolis force, shear and inertia of cross-section, inside pressure and the centrifugal force of the flow on transverse vibration of bellows are studied by both finite element and Hamilton's principle methods by using Timoshenko beam theory [11]. The investigation of the natural frequency of fluid-structure interaction in a fluid-conveying pipe is carried out using the eliminated element-Galerkin method. This method is used to derive natural frequency equations under various boundary conditions [12]. In this research paper we used the derived expression of comparison function, as is derived in mechanical vibration book written by S.S Rao [13].

In every areas of application of a pipeline usually works in the vibration environment. Such as, constrained ends of the penstock conveying water is excited by the water hammer effect or the earthquake, the fuel pipeline is positioned over an engine, alongside airborne pipes, and other fluid machinery parts. In this situation, the pipe supports are subject to external vibrations. This can result in the relaxation of constraints, potential pipe fatigue, and the risk of leakage in such conditions. This study examines the dynamic response

characteristics of a pipe, taking into account both the interaction between the fluid and structure, as well as the influence of externally induced vibrations on the supports. Initially, the dynamic equation for the pipeline with externally excited supports is derived using the Newtonian method, following the determination of fluid element accelerations as explained in the "Mathematical modelling" section. Subsequently, the Galerkin method is employed to construct a discrete dynamic model, and numerical analysis is conducted using the fourth order Runge-Kutta approach. Ultimately, the study explores the effects of fluid velocity and the frequency of external support-induced vibrations on the dynamic response of the pipe. The study includes an examination of pipes with two different end conditions, namely, those with pinned-pinned and pinned-free configuration.

2. Mathematical Modelling

The diagram of Pipe conveying fluid is as shown in Figure 1. The XOY coordinate system serves as the global inertial reference frame (unit vectors I and J). The local reference frame, xoy, is defined with respect to the supports is in reference to the supports (unit vectors i and j), as well as lateral velocity v_0, and lateral acceleration a_0. The measurement of lateral deflection w is conducted within the local xoy frame.

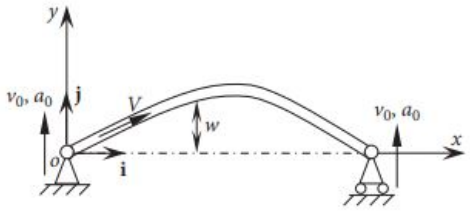

Figure 1: Schematics view of pipe conveying fluid

The fluid element's acceleration, is as shown in Figure 2, is needed to derive the governing dynamic equation of Pipe conveying fluid by the Newtonian approach. So, we present an additional moving reference frame $x'o'y'$, where (unit vectors i' and j'), which attached to the pipeline element. Parameters ϕ specify the slope angle of pipe cross-section and ρ specify the curvature radius of a deformed pipe element. By ignoring changes in the radial direction, we can represent the fluid element's acceleration as the acceleration of fluid particle at the point O'.

The dynamics composition theory can be used to express the fluid element's acceleration as follows:

$$a_f = a_r + a_e + 2\omega V, \tag{1}$$

where a_e, denoting convected acceleration, stands for the acceleration of point O' which is fixed in reference frame $x'o'y'$ in relation to the inertial reference frame i.e., XOY and a_r represents the relative acceleration, that is the acceleration fluid respective to the reference frame $x'o'y'$. The pipe cross section's angular velocity is represented by the ω, i.e, $\omega = (d\phi/dt)k'$, where k' is unit vector normal to the plane

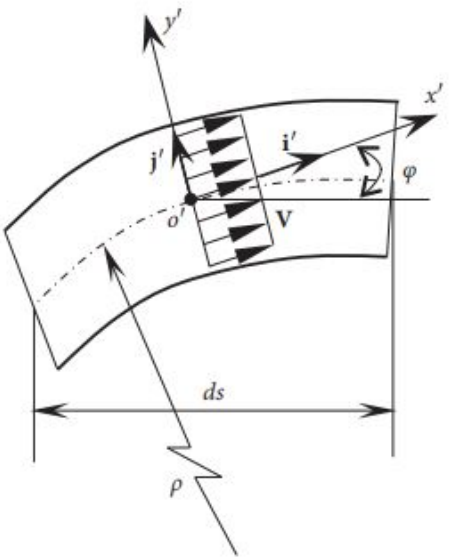

Figure 2: Fluid and pipe element

XOY outwards. $\mathbf{V}$, the fluid's velocity in the pipeline, i.s, $\mathbf{V} = Vi'$. The expression in Equation (1) is expressed as follows [1]:

$$a_r = \frac{dV}{dt}\mathrm{i}' - \frac{V^2}{\rho}\mathrm{j}', \tag{2}$$

$$a_e = \frac{\partial^2 \delta}{\partial t^2}\mathrm{i} + (a_0 + \frac{\partial^2 w}{\partial t^2})\mathrm{j} \simeq (a_0 + \frac{\partial^2 w}{\partial t^2})\mathrm{j}, \tag{3}$$

$$2\omega V = 2V\frac{d\phi}{dt}\mathrm{k}' \times \mathrm{i}' = 2V\frac{\partial^2 w}{\partial s \partial t}\mathrm{j}', \tag{4}$$

where δ is the longitudinal displacement, which is neglectable because it is the one order of magnitude smaller in compare to the lateral deflection w.
Substituting Equation (3) and $1/\rho = -(\partial^2 w/\partial s^2)/((1 + (\partial w/\partial s)^2)^3/2) \approx -\partial^2 w/\partial s^2$ into Equation (1), we have

$$a_f = \frac{\mathrm{d}V}{\mathrm{d}t}\mathrm{i}' + (2V\frac{\partial^2 w}{\partial s \partial t} + V^2\frac{\partial^2 w}{\partial s^2}\mathrm{j}') + (a_0 + \frac{\partial^2 w}{\partial t^2})\mathrm{j}. \tag{5}$$

Equation (5) is further simplified by the transformation relationship in between unit vectors i.e. i′, j′ and i, j. Since the pipe experiences only minor deformations, so the transformation is described in the following manner:

$$\begin{pmatrix}\mathrm{i}' \\ \mathrm{j}'\end{pmatrix} = \begin{pmatrix}\cos\varphi & \sin\varphi \\ -\sin\varphi & \cos\varphi\end{pmatrix}\begin{pmatrix}\mathrm{i} \\ \mathrm{j}\end{pmatrix} \approx \begin{pmatrix}1 & \frac{\partial w}{\partial s} \\ -\frac{\partial w}{\partial s} & 1\end{pmatrix}\begin{pmatrix}\mathrm{i} \\ \mathrm{j}\end{pmatrix} \tag{6}$$

The equation for fluid acceleration is given by substituting Equation (6) into Equation (5) while ignoring the second or higher level of infinitesimals, is as follows.

$$a_f = \frac{\mathrm{d}V}{\mathrm{d}t}\mathrm{i} + (\frac{\mathrm{d}V}{\mathrm{d}t}\frac{\partial w}{\partial s} + 2V\frac{\partial^2 w}{\partial s \partial t} + V^2\frac{\partial^2 w}{\partial s^2} + \frac{\partial^2 w}{\partial t^2} + a_0)\mathrm{j}. \tag{7}$$

Assuming that the pipe holds a constant flow of fluid and is not elongatable in the longitudinal direction, that is, s ≈ x and

also $dV/dt = 0$, Further simplification of Equation (7) can be expressed in the following manner:

$$a_f = (2V\frac{\partial^2 w}{\partial x \partial t} + V^2\frac{\partial^2 w}{\partial x^2} + \frac{\partial^2 w}{\partial t^2} + a_0)\text{j}. \quad (8)$$

Now the governing dynamic equation is derived with the

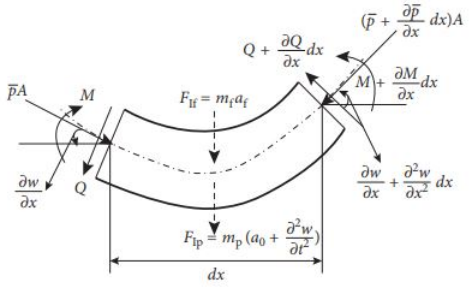

Figure 3: Schematic diagram of pipe element.

Newtonian method, after obtaining the fluid acceleration. The illustration in Figure 3 depicts the free body diagram of the pipe segment, where M and Q are bending moment and the transverse shear force. The pipe is having fluid pressure $\bar{p}$ and fluid flow area A. m_f is the the masses of fluid and m_p is the masses of pipe per unit length. Let F_{If}, denoted as the inertia force on the fluid and F_{Ip}, as inertia force on the pipe elements. Thus, the equation describing the lateral vibration motion of a fluid-conveying pipe can be presented as follows:

$$\frac{\partial Q}{\partial x} - \bar{p}A\frac{\partial^2 w}{\partial x^2} = F_{If} + F_{Ip} = m_f a_f + m_p(a_0 + \frac{\partial^2 w}{\partial t^2}). \quad (9)$$

By inserting the Equation (8) in Equation (9) and utilizing the connection between the shear force and the bending moment,that is, $(\partial Q/\partial x) = -(\partial^2 M/\partial x^2) = -(\partial^2/\partial x^2)(EI(\partial^2 w/\partial x^2))$, the equation of lateral vibration of motion is ultimately presented as follows:

$$EI\frac{\partial^4 w}{\partial x^4} + (m_f V^2 + \bar{p}A)\frac{\partial^2 w}{\partial x^2} + 2m_f V\frac{\partial^2 w}{\partial x \partial t} + (m_f + m_p)\frac{\partial^2 w}{\partial t^2} = -(m_f + m_p)a_0. \quad (10)$$

When the pipe ends vibrate as harmonically, i.e., $A_0 \sin\omega_0 t$,, where the acceleration is $a_0 = -A_0\omega_0^2 \sin\omega_0 t$, and resulting in the governing dynamic equation of the motion as follows:

$$EI\frac{\partial^4 w}{\partial x^4} + (m_f V^2 + \bar{p}A)\frac{\partial^2 w}{\partial x^2} + 2m_f V\frac{\partial^2 w}{\partial x \partial t} + (m_f + m_p)\frac{\partial^2 w}{\partial t^2} = -(m_f + m_p)A_0\omega_0^2 \sin\omega_0 t. \quad (11)$$

In order to make dimensionless, the subsequent dimensionless parameters are employed to derive the dimensionless version of the equation (11): $\eta = \frac{w}{L}$, $\xi = \frac{x}{L}$, $u = (\frac{M}{EI})^{1/2}LV$, $P = \frac{\bar{p}A}{EI}L^2$, $\beta = (\frac{m_f}{m_f+m_p})^{1/2}$, $\tau = (\frac{EI}{m_f+m_p})^{1/2}\frac{t}{L^2}$, $\omega = (\frac{m_f+m_p}{EI})^{1/2}\omega_0 L^2$, $\gamma = \frac{A_0}{L}$

where L is length of a pipe.
Ultimately, Equation of motion (11) takes on a dimensionless form as follows

$$\frac{\partial^4 \eta}{\partial \xi^4} + (u^2 + P)\frac{\partial^2 \eta}{\partial \xi^2} + 2\beta^{1/2}u\frac{\partial^2 \eta}{\partial \xi \partial \tau} + \frac{\partial^2 \eta}{\partial \tau^2} = \gamma\omega^2 \sin\omega\tau. \quad (12)$$

3. Dynamic Analysis

To deal with above equation of motion (12), galerkin method is applied. The dimensionless lateral deformation is denoted as follows:

$$\eta(\xi, \tau) \simeq \sum_{i=1}^{N} \phi_i(\xi) q_i(\tau), \quad (13)$$

Here, $\phi_i(\xi)$ is Comparison functions and assure the end condition, and $q_i(\tau)$ is the generalized coordinates of the discretized pipe structure. By inserting Equation (13) in Equation (12) and minimizing the residual value, we derive the subsequent discrete dynamic equation:

$$\text{M}\ddot{\text{q}} + \text{D}\dot{\text{q}} + \text{Kq} = \text{F}, \quad (14)$$

Where, Mass matrices $M_{ij} = \int_0^1 \phi_i(\xi)\phi_j(\xi)d\xi$, Damping matrices $D_{ij} = 2\beta^{1/2}u\int_0^1 \phi_i^{'}(\xi)\phi_j(\xi)d\xi$, Stiffness matrices $K_{ij} = \int_0^1 [\phi_i^{''''}(\xi) + (u^2 + P)\phi_i^{''}(\xi)]\phi_j(\xi)d\xi$, External Load $F_j = \int_0^1 \gamma\omega^2 \sin\omega\tau\phi_j(\xi)d\xi$, and $\dot{\text{q}}$ and $\ddot{\text{q}}$ are the generalized velocity and acceleration.

In order to solve Equation (14), the fourth order Runge–Kutta approach is used and take the following form:

$$\dot{\text{Y}}(\tau) = \text{AY}(\tau) + \text{P}(\tau), \quad (15)$$

where $\text{Y}(\tau) = \begin{pmatrix} \text{q}(\tau) \\ \dot{\text{q}}(\tau) \end{pmatrix}$, $\text{A} = \begin{pmatrix} 0_{N\times N} & \text{I}_{N\times N} \\ -\text{M}^{-1}\text{K} & -\text{M}^{-1}\text{C} \end{pmatrix}$, $\text{P}(\tau) = \begin{pmatrix} 0_{N\times 1} \\ \text{M}^{-1}\text{F} \end{pmatrix}$.
$I_{N\times N}$ is N-ordered identity matrix.
In the realm of numerical analysis, the dimensionless time step is defined as $\Delta\tau = 0.002$, and the initial conditions are given as $\text{q}(\tau) = \dot{\text{q}}(\tau) = 0$. As per Ni et al. [14], the convergence is achieved when galerkin truncation error in equation (13) set to $N \geq 4$ and we choose N= 4 for the subsequent analysis.

4. Model Validation

To demonstrate the efficiency of the proposed approach, we compare those results obtained through both analytical mode superposition method of classical beam problems and the newly suggested method in case of rubber pipe with pinned-pinned end conditions. The common parameters of pipe used for study are as tabulated in Table (1). In the case of a solid beam, it can be treated as a Pipe Conveying Fluid (PCF) with zero fluid velocity ($u = 0$) and no internal pressure ($\bar{p} = 0$). We will compare the results when is $u = 0$ as well as $\bar{p} = 0$. Equation (12) clearly represents the condition of a pipe with fixed supports under the influence of a uniform load as $p(\xi, \tau) = \gamma\omega^2 \sin(\omega\tau)$. In this scenario, as per beam theory [13], the lateral deflection of a pipe is formulated as in Equation (16).

$$\eta(\xi, \tau) = \sum \phi_i(\xi) q_i(\tau). \quad (16)$$

Now, by inserting Equation (17) into Equation (16), we can derive the analytical solution for the deflection of the pipe. We

observe that the outcomes obtained through the mode superposition method remain stable for $i \geq 3$. Therefore, we choose $i = 4$ for the purpose of comparison. The results obtained through the two methods, closely align with each other as shown in Figure (4). Thus, the validation of the proposed method is confirmed.

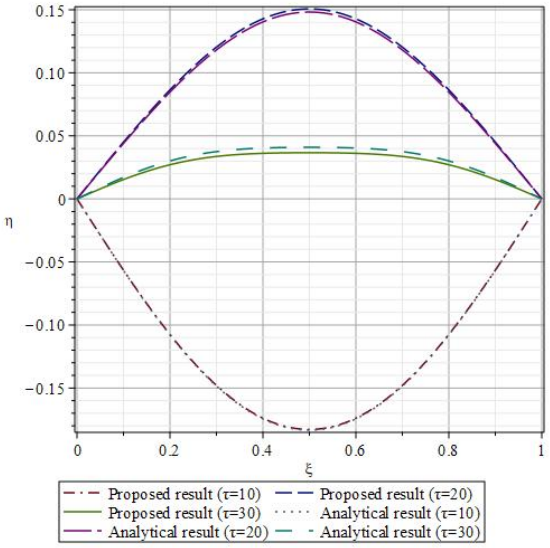

Figure 4: Comparing the deflection of the pipe with pinned ends using two methods

5. Results and Discussion

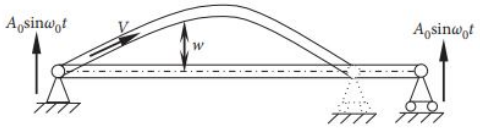

Figure 5: Pinned-pinned pipe end condition

In this section, two different materials pipes are analyzed and results are compared. Pipes with two end conditions: pinned-pinned, and pinned-free are studied. In each end conditions two different materials are studied in respect of deflection and bending moment.

The parameters employed for model validation are also utilized in the numerical analysis are as tabulated in Table (1).

Table 1: Parameters for Study

SN	Parameters	Values
1	Length of pipe	0.362m
2	Outside diameter of pipe	9.7mm
3	Inside diameter of pipe	6mm
4	Density of water	1000 kg/m^3
5	Mean inner Pressure($\bar{P}$)	2 MPa

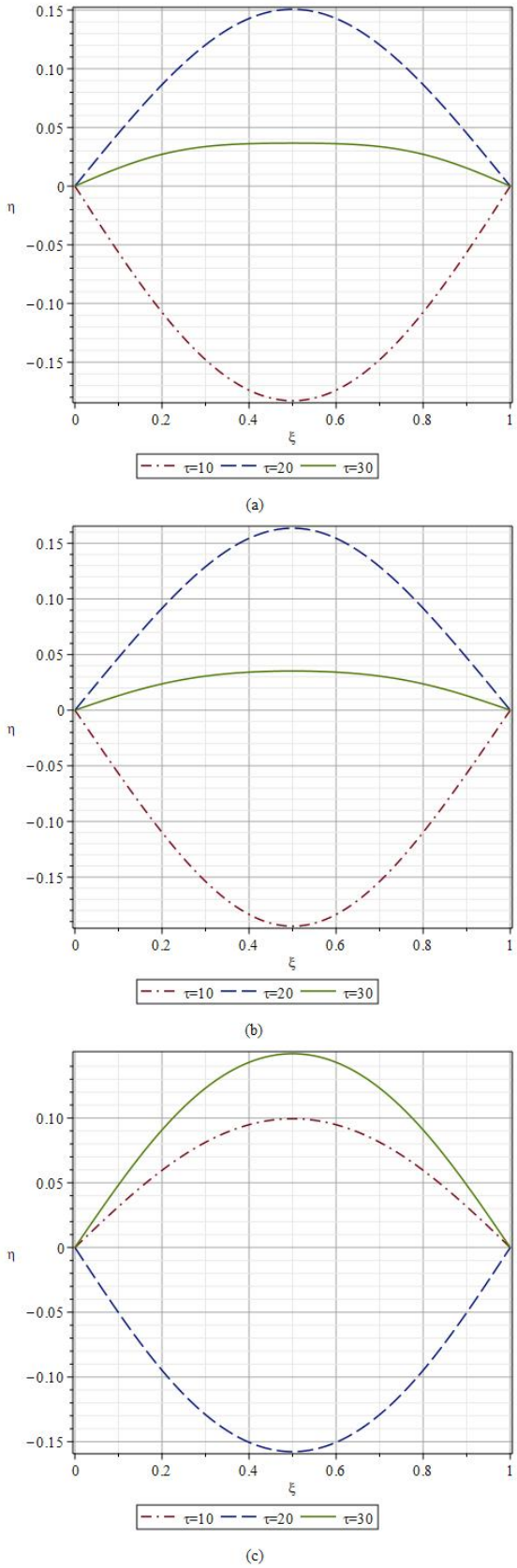

Figure 6: The deflections of the rubber pipe with pinned-pinned ends at various fluid velocities: (a) when u=0, (b) when u=1, and (c) when u=2

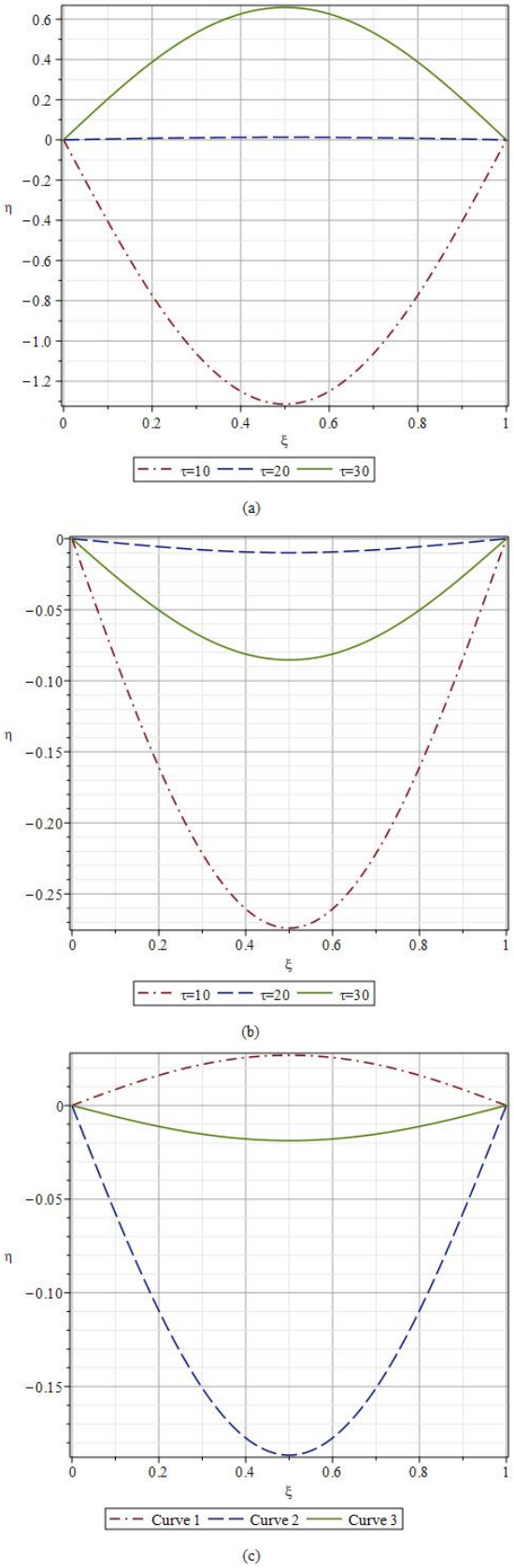

Figure 7: The deflections of the steel pipe with pinned-pinned ends at various fluid velocities:(a) when u=0 (b) when u=1, and (c) when u=2

The supports undergo harmonic motion, i.e., $A_0 \sin(\omega_0 t)$, with amplitude of $A_0 = 0.012m$ and angular frequency of $\omega_0 = 488.28\pi rad/s$. Young's modulus of elasticity for Rubber and steel are taken as 2.924 GPa and 207 GPa respectively. Density of steel as well as rubber are 8000 kg/m^3 and 1128.56 kg/m^3 respectively. Similarly total mass per unit length of steel and rubber is 0.36 kg/m and 0.05 kg/m respectively.

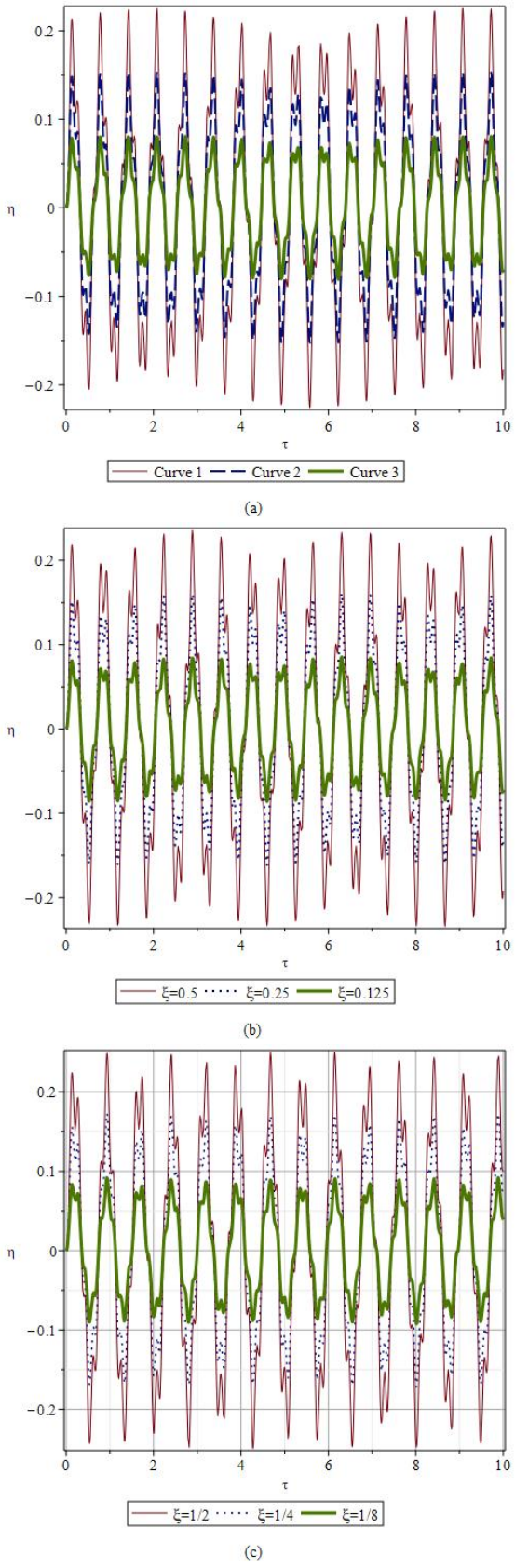

Figure 8: The deflections at various points along the rubber pipe with pinned-pinned ends under different fluid velocities: (a)when u=0, (b) when u=1, and (c) when u=2

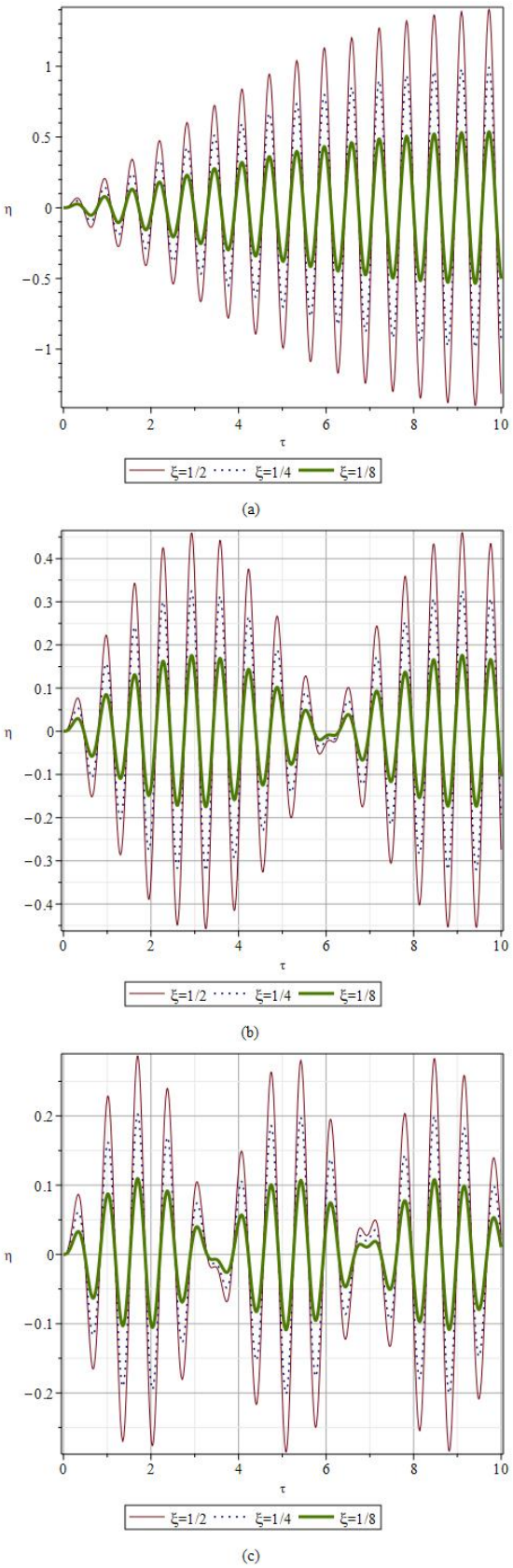

Figure 9: The deflections at various points along the steel pipe with pinned-pinned ends under different fluid velocities: (a)when u=0, (b) when u=1, and (c) when u=2

5.1 The Pinned-Pinned end condition

As per beam theory, comparison function for the pinned-pinned pipeline, is shown as in Figure 5, is $\phi_i(\xi) = \sin(i\pi\xi)$. Assuming the uniform an external load $p(\xi,\tau) = \gamma\omega^2 \sin\omega\tau$ and the initial condition, that is, $\eta(\xi,0) = 0$, $\dot{\eta}(\xi,0) = 0$. Likewise, it is possible to express the generalized coordinate analytically [13] as in equation (17). Here, ω_i represents the ith natural frequency of the pipe with pinned-pinned ends.

To compute the deflection, the first four natural frequency modes are determined using the wave approach method initially introduced by Li et al. [12]. The natural frequencies results are tabulated in Table (2).

$$\begin{aligned} q_i(\tau) &= (1-(-1)^i)\frac{1}{\omega_i}\frac{2\gamma\omega^2}{i\pi}\int_0^\tau \sin\omega\zeta \sin\omega_i(\tau-\zeta)d\zeta \\ &= \frac{2\gamma\omega^2}{i\pi}\frac{(1-(-1)^i)}{\omega_i^2}(\sin\omega\tau - \frac{\omega}{\omega_i}\sin\omega_i\tau) \end{aligned} \tag{17}$$

Table 2: The dimensionless first four modes of natural frequencies of the pinned-pinned Pipe end condition.

u	ω_1	ω_2	ω_3	ω_4
0	9.86	39.44	88.79	157.87
1	9.23	38.57	87.62	156.52
2	8.42	36.33	86.35	155.46

The three deflection curve modes shown in Figure 6 and Figure 7 vary for each scenario. Here, deflection graphs as in Figures 6(b) and 6(c) for rubber material pipe and the deflection graphs in Figures 7(b) and 7(c) for steel material pipe, resemble each other because of the fluid flow inside the pipe. The graphs in Figure 6 and 7 illustrate that deflections progressively rise as fluid velocity increases. This indicates that as the fluid velocity increases, the flexural rigidity of a pipe diminishes. The impact is also evident in the natural frequencies of pipe under varying fluid velocities.

Similarly, Figure 8 and 9 depict the deflection curves of the pipe at various positions ($\xi = 1/2$, and $\xi = 1/4$, and $\xi = 1/8$) under different fluid velocities ($u = 0$, and $u = 1$, and $u = 2$). Figure 8 for rubber material pipe and figure 9 for steel material pipe implies that the deflection's magnitude grows with the fluid velocity. The greatest deflection is observed at the pipe's midpoint. The deflection of a point diminishes as the point approaches either end of the pipe. As the fluid velocity rises, the response curves become progressively more scattered. This suggests that the time it takes for the response to occur increases, indicating a reduction in natural frequency.

Another dynamic response, bending moment, for the pipe can be analysed through following dimensionless bending moment:

$$\bar{M} = \frac{ML}{EI} = \frac{\partial^2\eta}{\partial\xi^2} \tag{18}$$

Figure 10 and 11 shows curves of bending moment on the pinned-pinned of rubber and steel pipe at three distinct positions along the pipe ($\xi = 1/2$, and $\xi = 1/4$, and $\xi = 1/8$) in relation to three varying fluid velocities ($u = 0$, and $u = 1$, and $u = 2$).

In Figure 11(a), at a fluid velocity of ($u = 0$), the bending moment at ($\xi = 1/2$) is greater than that at ($\xi = 1/4$) and

(ξ = 1/8), but the bending moments are at (ξ = 1/4) and (ξ = 1/8) exhibit only a slight difference. As the fluid velocity increases, the bending moments at all three positions also increase concurrently.

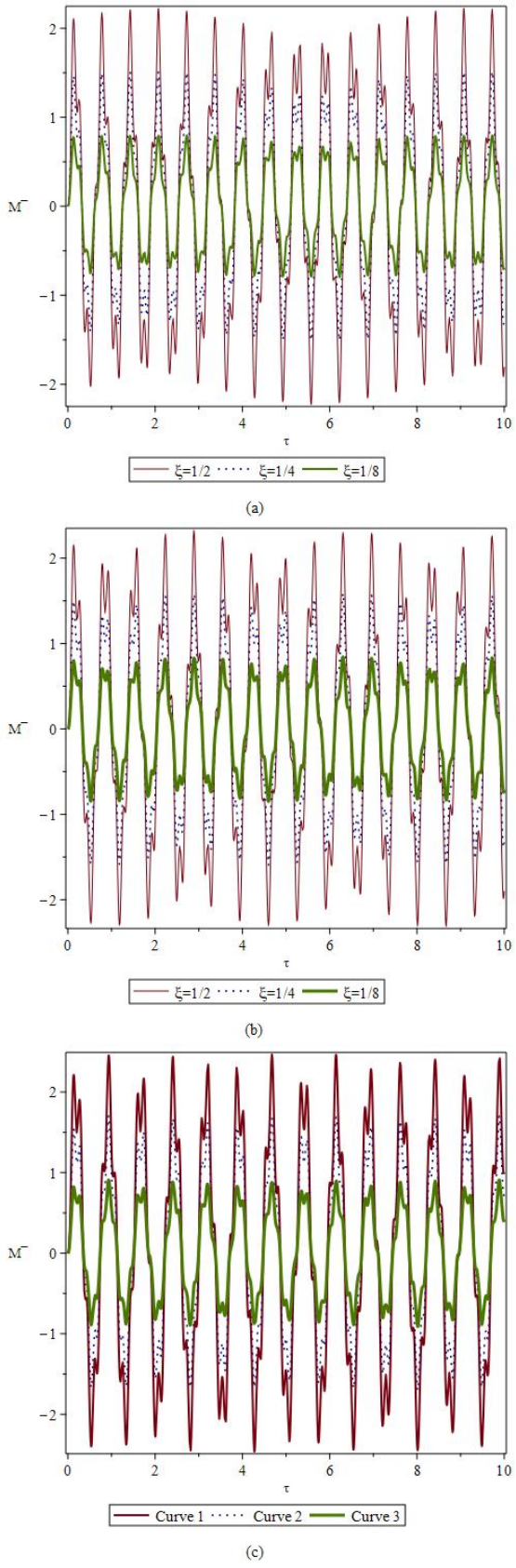

Figure 10: The bending moments at various positions along the rubber pipe with pinned-pinned ends under different fluid velocities: (a) when u=0, (b) when u=1, and (c)when u=2

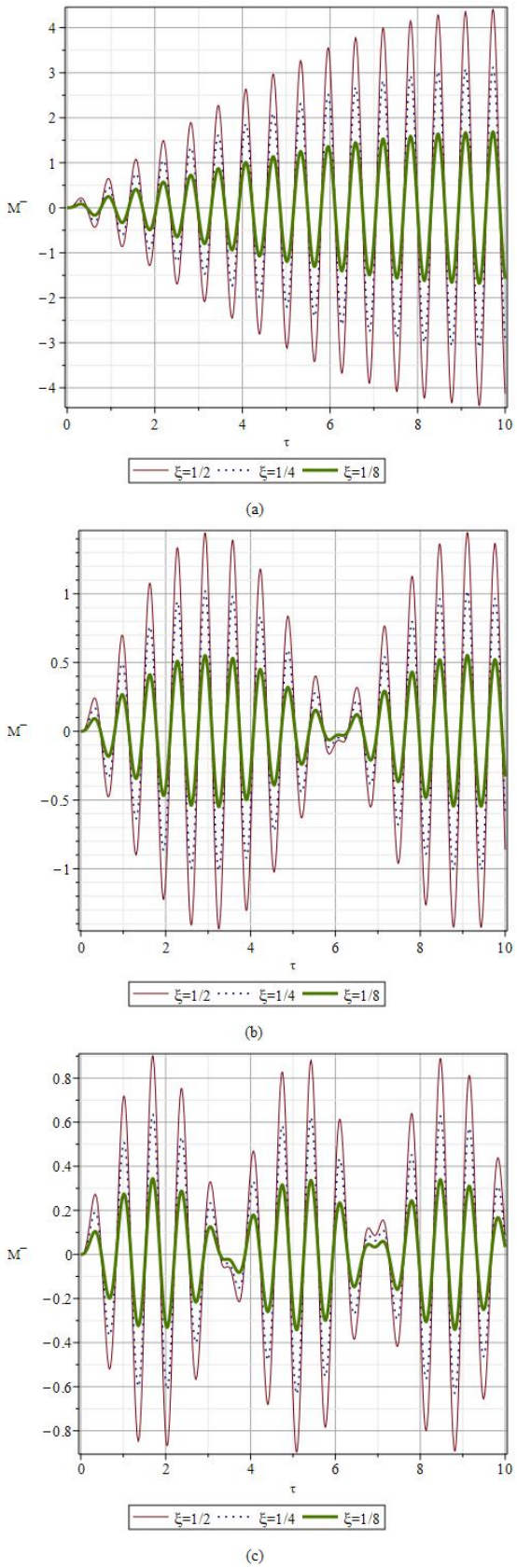

Figure 11: The bending moments at various positions along the steel pipe with pinned-pinned ends under different fluid velocities: (a) when u=0, (b) when u=1, and (c) when u=2

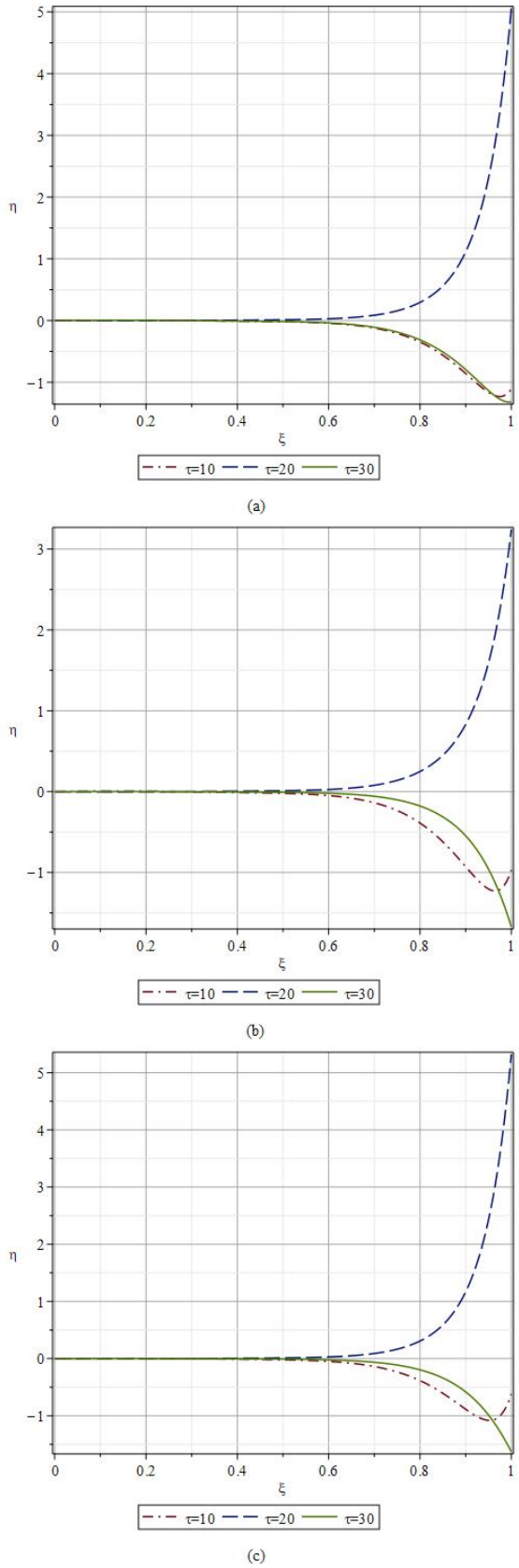

Figure 12: The deflections of the pinned-free ends of rubber pipe with various fluid velocities:(a) when u=0 (b)when u=1 (c) when u=2

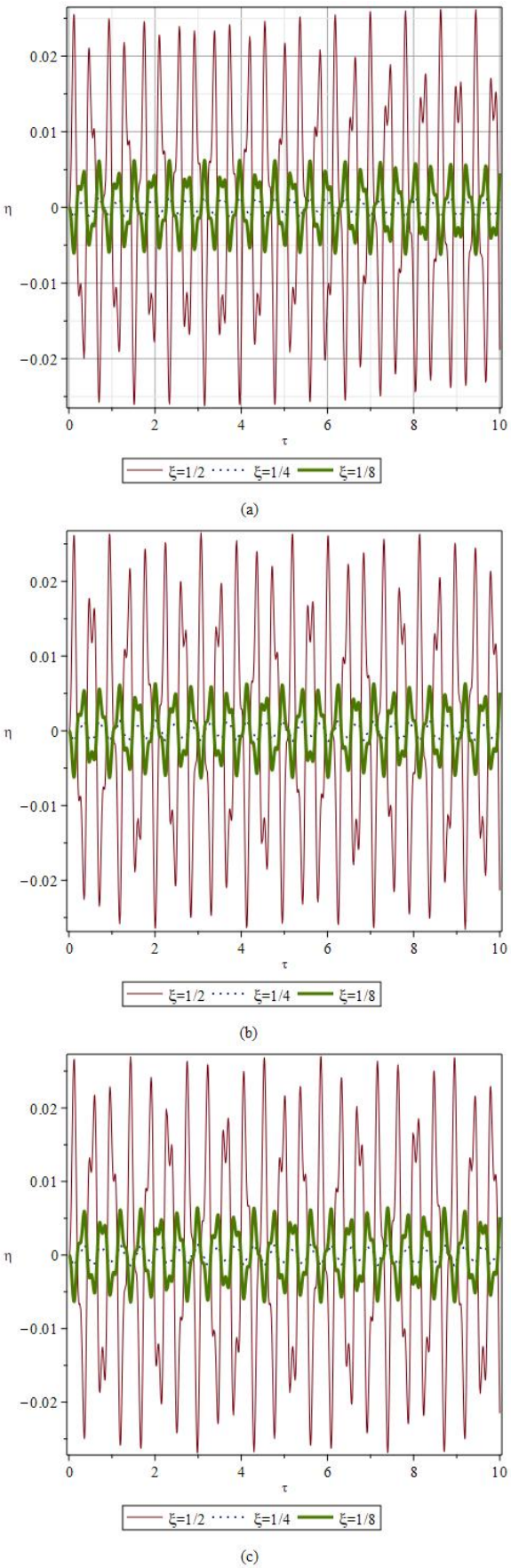

Figure 13: The deflections at various points along the rubber pipe with pinned-free ends under different fluid velocities: (a) when u=0, (b) when u=1, and (c)when u=2

5.2 The Pinned-Free end condition

A different category of fluid-carrying pipe is one with pinned-free end condition whose comparison function is given by [13] as follows:

$$\phi_i(\xi) = \sin\beta_i\xi + \alpha_i sinh\beta_i\xi, \tag{19}$$

where $\alpha_i = \frac{\sin\beta_i l}{sinh\beta_i l}$ and $\beta_i l = (i + 1/4)\pi$ as when $i \geq 1$. The values of $\beta_i l$ are tabulated in Table 3 [13].

Table 3: The values of $\beta_i l$ for pinned-free pipe conveying fluid.

$\beta_1 l$	$\beta_2 l$	$\beta_3 l$	$\beta_4 l$
3.9366	7.786	10.1102	13.4518

The deflection responses of pipe under three different velocities of fluid ($u = 0$, and $u = 1$, and $u = 2$) are depicted at three distinct time points ($\tau = 10$, and $\tau = 20$, and $\tau = 30$) is as shown in Figure 12. None of the cases in Figure 12 exhibit a symmetric mode because of the asymmetric supports. The deflection of a pipe does not change consistently with the velocity of fluid. At time when $\tau = 10$, as the velocity of fluid increases, the deflection initially rises and subsequently decreases. Nevertheless, at $\tau = 20$, the deflection consistently increases.At $\tau = 30$, the deflection initially exhibits a decrease and then subsequently rise.

Figure 13 shows the deflection curves of the pipe with pinned-free ends, conveying fluid, at various positions ($\xi = 1/2$, and $\xi = 1/4$, and $\xi = 1/8$), and under different fluid velocities ($u = 0$, and $u = 1$, and $u = 2$). It can be noted that deflections increase as fluid velocity rises. Nonetheless, when compared to the pinned-pinned pipe, the pinned-free pipe exhibits a smaller fluctuation in deflection. This difference is primarily attributed to one end being pinned while the other is free in the pinned-free pipe, resulting in a lesser impact on the pipe's deflection by the same fluid velocity.

Likewise, Figure 14 presents the graphs of bending moment for the pinned-free pipe under various scenarios. Figure 14 reveals that, in each instance, the highest bending moment on a pinned-free pipe occurs at $\xi = 1/2$, consistent with the behavior of a pinned-pinned pipe. Nevertheless, the bending moment at position $\xi = 1/8$ is greater than the bending moment at position $\xi = 1/4$, which differs from the behavior of the pinned-pinned pipe. The bending moment on the pinned-pinned pipe is considerably smaller than that on the pinned-free pipe.

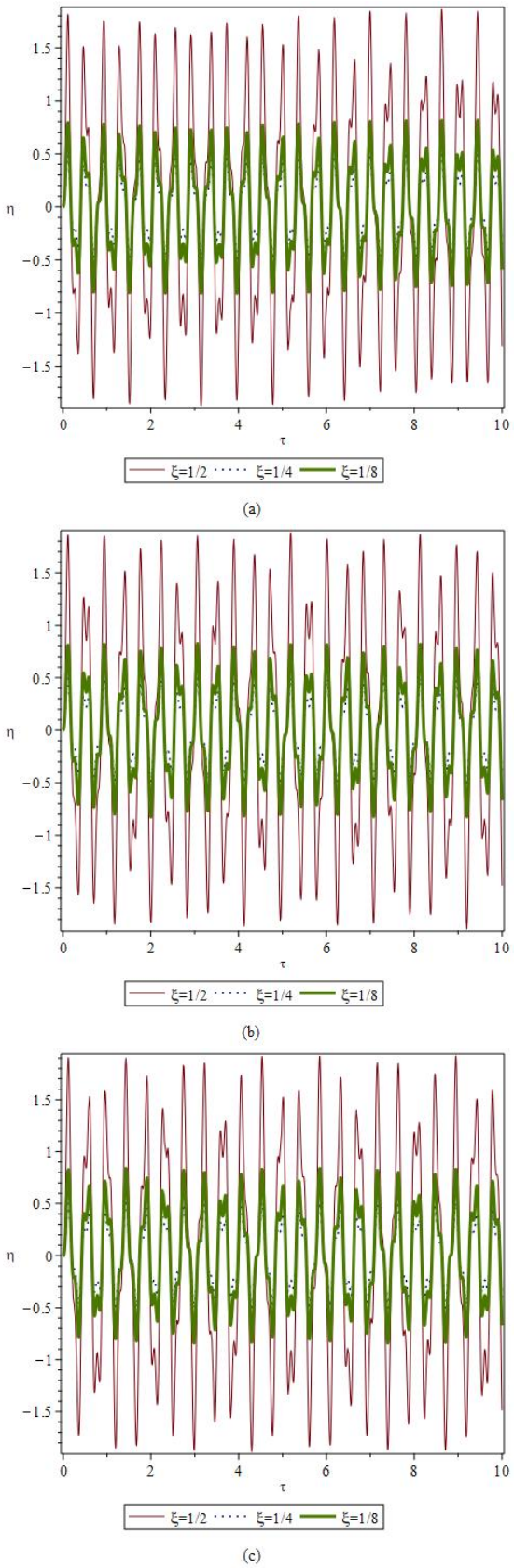

Figure 14: The bending moment at various points along the pinned-free pipe under various fluid velocities:(a) when u=0 (b) when u=1 (c)when u=2

6. Conclusions

This study explores the dynamic behaviors of fluid-conveying pipes made of rubber and steel with pinned-pinned and pinned-free end conditions, subjected to excited supports. The paper derives dynamic equations using the Newtonian method after calculating fluid acceleration. Numerical analysis is conducted using the Galerkin method and fourth-order Runge-Kutta method. The study investigates deflection and bending moment responses under various fluid velocities and materials. The conclusions are made as follows:

1. The deflection as well as bending moment increases with fluid velocities. This suggests that as the fluid speed increases, the pipe's stiffness decreases.

2. The largest deflection occurs on a pinned-pinned pipe seen at position ($\xi = 1/2$). The deflection at position $\xi = 1/4$ as well as $\xi = 1/8$ is less difference in comparison, which is not in accordance of the fluid velocity. The deflection is more in Rubber pipe in compare to steel pipe with given same parameters.

3. The bending moment magnitudes for both pinned-pinned and pinned-free pipes follow the order $\bar{M}(\xi = 1/2) > \bar{M}(\xi = 1/8) > \bar{M}(\xi = 1/4)$ when the fluid is at a standstill. However, as fluid velocity increases, it is observed that bending moment at position $\xi = 1/4$ increases quickly and approaches a magnitude close to that at position $\xi = 1/8$.

4. The impact is also evident in the natural frequencies of the pipe at varying fluid velocities.

Acknowledgments

The authors express their appreciation to Er. Sunil Adhikari, Er. Raj Kumar Chaulagain, and Er. Manoj Dangal for their valuable technical assistance and guidance throughout the research project. This research project could not have been accomplished without their assistance.

References

[1] M. P. Paıdoussis, fluid–structure interactions: Slender structures and axial flow, vol. 1. 1998.

[2] MP Paıdoussis and GX Li. Pipes conveying fluid: a model dynamical problem. *Journal of fluids and Structures*, 7(2):137–204, 1993.

[3] R.A. Ibrahim. Overview of mechanics of pipes conveying fluids—part i: Fundamental studies. *Journal of Pressure Vessel Technology*, 132(3):1–32, 2010.

[4] M Kheiri and MP Païdoussis. On the use of generalized hamilton's principle for the derivation of the equation of motion of a pipe conveying fluid. *Journal of Fluids and Structures*, 50:18–24, 2014.

[5] DB McIver. Hamilton's principle for systems of changing mass. *Journal of Engineering Mathematics*, 7(3):249–261, 1973.

[6] Ivan Grant. *Flow induced vibrations in pipes, a finite element approach.* PhD thesis, Cleveland State University, 2010.

[7] YL Zhang, DG Gorman, and JM Reese. Analysis of the vibration of pipes conveying fluid. *Proceedings of the Institution of Mechanical Engineers, Part C: Journal of Mechanical Engineering Science*, 213(8):849–859, 1999.

[8] S. Naguleswaran and C.J.H Williams. Lateral vibration of a pipe conveying a fluid. *Journal of Mechanical Engineering Science*, 10(3):228–238, 1968.

[9] Huang Yi-min, Ge Seng, Wu Wei, and He Jie. A direct method of natural frequency analysis on pipeline conveying fluid with both ends supported. *Nuclear Engineering and Design*, 253:12–22, 2012.

[10] Huang Yi-Min, Liu Yong-Shou, Li Bao-Hui, Li Yan-Jiang, and Yue Zhu-Feng. Natural frequency analysis of fluid conveying pipeline with different boundary conditions. *Nuclear Engineering and Design*, 240(3):461–467, 2010.

[11] Feliksas Vaidutis Jakubauskas. Transverse vibrations of bellows expansion joints. 1995.

[12] Huang Yi-Min, Liu Yong-Shou, Li Bao-Hui, Li Yan-Jiang, and Yue Zhu-Feng. Natural frequency analysis of fluid conveying pipeline with different boundary conditions. *Nuclear Engineering and Design*, 240(3):461–467, 2010.

[13] Singiresu S Rao. Mechanical vibrations, prentice hall. *Indianapolis, IN*, 2011.

[14] Qiao Ni, Yangyang Luo, Mingwu Li, and Hao Yan. Natural frequency and stability analysis of a pipe conveying fluid with axially moving supports immersed in fluid. *Journal of Sound and Vibration*, 403:173–189, 2017.